

Percolation conductivity in hafnium sub-oxides

D. R. Islamov,^{1,2, a)} V. A. Gritsenko,^{1,2, b)} C. H. Cheng,³ and A. Chin^{4, c)}

¹⁾*Rzhanov Institute of Semiconductor Physics, Siberian Branch of Russian Academy of Sciences, Novosibirsk, 630090, Russian Federation*

²⁾*Novosibirsk State University, Novosibirsk, 630090, Russian Federation*

³⁾*Dept. of Mechatronic Technology, National Taiwan Normal University, Taipei, 106, Taiwan ROC*

⁴⁾*National Chiao Tung University, Hsinchu, 300, Taiwan ROC*

(Dated: 27 August 2018)

In this study, we demonstrated experimentally that formation of chains and islands of oxygen vacancies in hafnium sub-oxides (HfO_x , $x < 2$) leads to percolation charge transport in such dielectrics. Basing on the model of Éfros-Shklovskii percolation theory good quantitative agreement between the experimental and theoretical data of current-voltage characteristics were achieved. Based on the percolation theory suggested model shows that hafnium sub-oxides consist of mixtures of metallic Hf nanoscale clusters of 1–2 nm distributed onto non-stoichiometric HfO_x . It was shown that reported approach might describe low resistance state current-voltage characteristics of resistive memory elements based on HfO_x .

PACS numbers: 77.55.df, 77.84.Bw, 72.80.Ng, 72.20.–i

Keywords: hafnium oxides, metal-insulator-metal (MIM), percolation theory, potential fluctuations

Hafnium oxide (hafnia, HfO_2) and sub-oxides (HfO_x , $x < 2$) play extremely important roles in modern micro-electronics. Hafnia is used in modern MOSFETs as high- κ gate dielectric with low leakage currents^{1–4}. Hafnium sub-oxides are the most promising materials to be used as active medium in resistive random access memory (RRAM)^{5,6}, which might be used for universal memory combining the most favorable properties of both high-speed dynamic random access memory, and non-volatile flash memory^{7–11}. RRAM has many advantages: a simple metal-insulator-metal (MIM) structure, a small memory cell, potential for 3D integration, high read and write operation speeds, low power consumption, and the ability to store information over the long term. A RRAM operation is principally based on switching back and forth from the insulating medium's high resistance state (HRS) to a low resistance state (LRS) when a current flows. Conductivity of HfO_x used as RRAM active medium is limited by ionization of charge carrier traps when RRAM is switched to the HRS state^{6,12,13}. Unfortunately, unlike the flash memory, the fundamental physics mechanism of RRAM is still inadequate, but that is vital to realize the ultra-low-power memory array.

In this letter, we report that the charge transport mechanism is described in terms of percolation theory when hafnium-sub-oxides-based RRAM is switched to the LRS state.

Transport measurements were recorded for MIM structures of Si/TaN/ HfO_x /Ni. To fabricate these structures, we deposited the 8-nm-thick amorphous HfO_x on 100-nm-thick TaN films on Si wafers, using physical vapor

deposition. A pure HfO_2 target was bombarded by an electron beam, and HfO_2 was deposited on the wafer. No post deposition annealing was applied to produce highly non-stoichiometric HfO_x films. Structural analysis showed that the resulting films were amorphous. All samples for transport measurements were equipped with round 50-nm-thick Ni gates with a radius of 70 μm .

Transport measurements were performed using a Hewlett Packard 4155B Semiconductor Parameter Analyzer and an Agilent E4980A Precision LCR Meter. All measurement equipment were protected against short circuiting with the current through the sample limitation of 1 μA .

The most commonly used LRS description in RRAM structures consists of conductive filament (CF), approximately 1–10 nm in diameter (D)^{14–16}. The CF forming is cause by charged ion movements due to temperate gradients and electric fields¹⁶. It was supposed, that CFs in Ni/ HfO_2 /Si RRAM structures consist of nickel, migrated from the metal electrode¹⁵, but these assumptions were based on results of RRAM measurements in Ni/NiO/Ni-type structures (i.e. with NiO dielectric medium with Ni electrodes). However, CF has metallic temperature dependence of resistance

$$(R - R_0) \propto (T - T_0) \quad (1)$$

(here R_0 is the CF resistance at temperature T_0), with average resistivity in three order smaller than resistivity of pure Hf metal¹⁴.

Assuming, that the current-voltage characteristics (I - V) are described by Ohm's law, we compared calculated I - V for Hf metal wire 8 nm long with diameters of 10 nm (dashed light green line in Fig. 1), 1 nm (dashed with dots dark green line in Fig. 1), and sub-stoichiometric HfO_x CF¹⁴ ($D = 1$ nm, dark cyan dotted line in Fig. 1) with experiment results, indicated by the colored characters in

^{a)}Electronic mail: damir@isp.nsc.ru

^{b)}Electronic mail: grits@isp.nsc.ru

^{c)}Electronic mail: albert.achin@hotmail.com

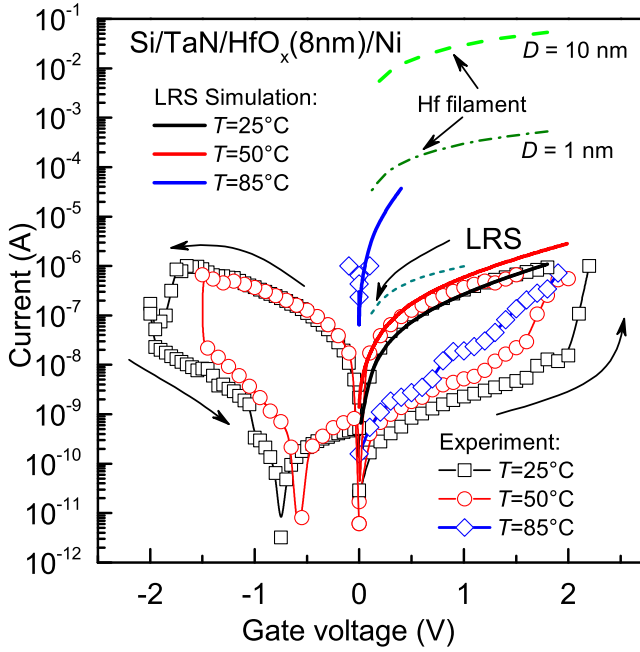


FIG. 1. (Color online) Experimental RRAM current-voltage characteristics hysteresis (characters) in Si/TaN/HfO_x/Ni MIM structures at different temperatures. Black, red and blue solid lines present LRS simulations in terms of percolation model. Green lines model current-voltage characteristics of pure Hf CF of length of 8 nm and diameter of 1 nm and 10 nm; dark cyan dotted line models I - V of sub-stoichiometric HfO_x CF with diameter of 1 nm.

Fig. 1. Calculated values of the current through pure Hf wires are 10^3 – 10^5 times higher than the values obtained in the experiments. Furthermore, such a high current cannot be used for large memory arrays because of high power consumption¹⁷. We understand, that a cylinder shape of the metal filament is not accurate model of CF, however we used these estimations as motivations for further research. The current through non-stoichiometric HfO_x CF is close to experiment results, but expected values are large for temperatures of $T = 25$ – 50°C , and lower than measured at $T = 85^\circ\text{C}$. The current grows exponentially with temperature growing, while following results from the literature, the current should decrease with the temperature increasing (1).

Therefore, we suppose that LRS conductivity is conditioned by the presence of a non-stoichiometric HfO_x islands in HfO₂ matrix as HfO_y with $y \lesssim 1.89$ splits into phases of Hf, HfO_x and HfO₂¹⁸. The overview on the structure of non-stoichiometric sub-oxides and sub-nitrides was developed for SiO_x, SiN_x, and SiO_xN_y^{19–22}.

A 2D structural image of non-stoichiometric HfO_x, regarding the intermediate structural model²⁰, is presented in Fig. 2(a). According to this model, the CF in hafnium sub-oxide consists of a mixture of metallic hafnium nanoscale clusters (blue drops) and non-stoichiometric HfO_x (green islands) distributed onto HfO₂ matrix (yel-

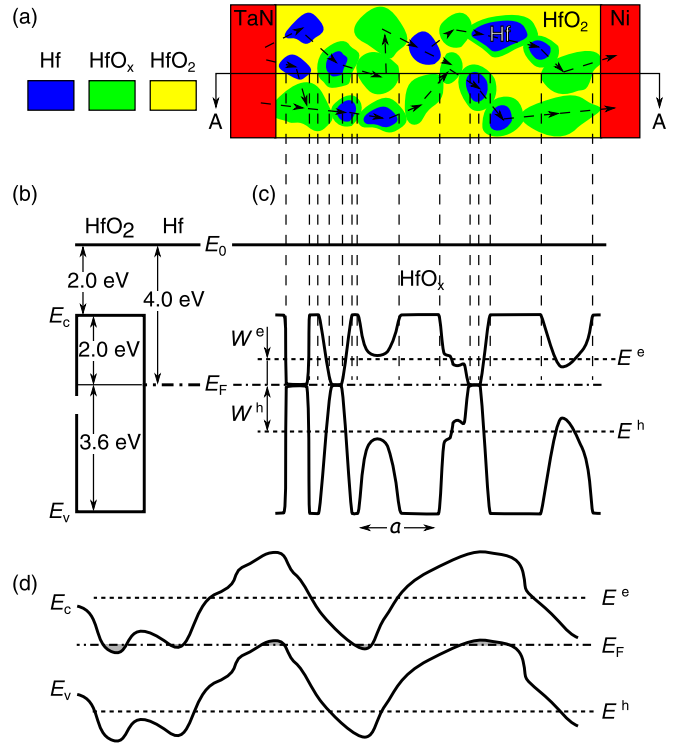


FIG. 2. (Color online) Percolation model in electron systems with the nanoscale potential fluctuations. (a) Schematic planar illustration of Hf/HfO_x ($x < 2$) space-modulated by chemical composition structure. (b) Flat band energy diagram of HfO₂/Hf structure. (c) Energy diagram of the structure with nanoscale potential fluctuations. (d) Energy diagram of large-scale potential fluctuations in a semiconductor layer²⁴. $E^{e,h}$ and $W^{e,h}$ are percolation levels and percolation thresholds of the electrons and holes respectively.

low area). Fig. 2(c) is an energy diagram of HfO_x in the intermediate structural model. According to this plot, spatial fluctuations in the chemical composition of HfO_x lead to local band gap width spatial fluctuations. The maximal fluctuation of the energy scale is equal to the HfO₂ band gap width of $E_g = 5.6\text{ eV}$ ²³. The work function of metallic hafnium is 4.0 eV. The maximal fluctuation scale of the HfO_x conduction band is 2.0 eV, which equals the electron barrier height of Hf/HfO₂ interface. The hole energy barrier of Hf/HfO₂ is 3.6 eV (Fig. 2(b)), which leads to the maximal fluctuation scale of the HfO_x valence band of 3.6 eV.

The nanoscale fluctuations at the bottom of conduction band E_c and at the top of valence band E_v are close to those proposed in the model developed in^{24,25}, as shown in Fig. 2(d). The charge transport in such electron systems can be described according to percolation. This model assumes that excited electrons with energy higher than the flow level E^e are delocalized, and driving round a random potential, transfer the charge. The hole conductivity is realized through the excitation of electrons with energy E^h to the Fermi level. These excitations form

hole-type quasiparticles, which transfer the charge. In other words, to be involved in transport processes, electrons and holes must overcome energy thresholds ($W^{e,h}$ here, and $W^e \neq W^h$ in general). The current-voltage characteristics are exponentials²⁴:

$$I(T) = I_0(T) \exp\left(\frac{(CeFaV_0^\nu)^{\frac{1}{1+\nu}}}{kT}\right), \quad (2)$$

where I is the current, I_0 is the preexponential factor, e is the electron charge, F is the electric field, a is the space scale of fluctuations, V_0 is the amplitude of energy fluctuation, k is the Boltzmann constant, C is a numeric constant, and ν is a critical index. The values of the constants were derived from Monte-Carlo simulations and evaluated at $C \simeq 0.25$ ²⁴ and $\nu = 0.9$ ²⁵. Percolation energy threshold W can be evaluated based on the temperature dependency of the preexponential factor:

$$I_0(T) \sim \exp\left(-\frac{W}{kT}\right). \quad (3)$$

The solid colored lines in Fig. 1 indicate the results of LRS simulations regarding the percolation model, given in (2). Numeric fitting returns the value of combination as $CaV_0^{0.9} = 0.45 \text{ nm} \cdot \text{eV}^{0.9}$, which corresponds to $V_0 = 1.9 \text{ eV}$ when $a = 1 \text{ nm}$ and $C = 0.25$. The slope of a fitting line in a $\ln(I_0)$ -vs- T^{-1} plate according to (3) corresponds to a percolation threshold of $W \approx 1.0 \text{ eV}$. Because $W \lesssim V_0 \leq 2.0 \text{ eV}$ (for electrons), we can estimate the space size of nanoscale fluctuations as $a \approx 1\text{--}2 \text{ nm}$.

Previous experiments in charge transfer have demonstrated that hafnia conductivity is bipolar (or two-band)^{4,26–28}: electrons are injected from a negatively shifted contact in the dielectric, and holes are injected from a positively shifted electrode in the dielectric. In our model, LRS conductivity can also be studied using electrons and holes. For the reason of simplicity, the current study was limited to considering monopolar electron conductivity.

The results demonstrate that charge transport in non-stoichiometric hafnium sub-oxides is described according to the percolation model in electron systems exhibiting potential nanoscale fluctuations. This approach can be applied to explain RRAM in GeO_x - and SiO_x -based structures^{29,30}.

This work was partly supported by National Science Council, Taiwan (grant No. NSC103-2923-E-009-002-MY3) (growing test structures, preparing samples, and performing transport measurements), and by the Russian Science Foundation (grant No. 14-19-00192) (calculations and modeling).

¹Z. Xu, M. Houssa, R. Carter, M. Naili, S. D. Gendt, and M. Heyns, *Journal of Applied Physics* **91**, 10127 (2002).

- ²T. P. Ma, H. M. Bu, X. W. Wang, L. Y. Song, W. He, M. Wang, H.-H. Tseng, and P. J. Tobin, *IEEE Trans. Device Mater. Rel.* **5**, 36 (2005).
- ³J. Robertson, *Reports on Progress in Physics* **69**, 327 (2006).
- ⁴L. Vandelli, A. Padovani, L. Larcher, R. G. Southwick, W. B. Knowlton, and G. Bersuker, *IEEE Trans. Electron Devices* **58**, 2878 (2011).
- ⁵L. Goux, P. Czarnecki, Y. Y. Chen, L. Pantisano, X. P. Wang, R. Degraeve, B. Govoreanu, D. J. Jurczak, M. and Wouters, and L. Altimime, *Applied Physics Letters* **97**, 243509 (2010).
- ⁶Z. Wang, H. Y. Yu, X. A. Tran, Z. Fang, J. Wang, and H. Su, *Physical Review B* **85**, 195322 (2012).
- ⁷D. B. Strukov, G. S. Snider, D. R. Stewart, and R. S. Williams, *Nature* **453**, 80 (2008).
- ⁸J. J. Yang, M. D. Pickett, X. Li, D. A. A. Ohlberg, D. R. Stewart, and R. S. Williams, *Nature Nanotechnology* **3**, 429 (2008).
- ⁹M.-J. Lee, S. Han, S. H. Jeon, B. H. Park, B. S. Kang, S.-E. Ahn, K. H. Kim, C. B. Lee, C. J. Kim, I.-K. Yoo, D. H. Seo, X.-S. Li, J.-B. Park, J.-H. Lee, and Y. Park, *Nano Letters* **9**, 1476 (2009).
- ¹⁰J. Borghetti, G. S. Snider, P. J. Kuekes, J. J. Yang, D. R. Stewart, and R. S. Williams, *Nature* **464**, 873 (2010).
- ¹¹M.-J. Lee, C. B. Lee, D. Lee, S. R. Lee, M. Chang, J. H. Hur, Y.-B. Kim, C.-J. Kim, D. H. Seo, S. Seo, U.-I. Chung, I.-K. Yoo, and K. Kim, *Nature Materials* **10**, 625 (2011).
- ¹²S. D. Ganichev, E. Ziemann, W. Prettl, I. N. Yassievich, A. A. Istratov, and E. R. Weber, *Phys. Rev. B* **61**, 10361 (2000).
- ¹³D. R. Islamov, V. A. Gritsenko, C. H. Cheng, and A. Chin, *Applied Physics Letters* **105**, 222901 (2014), arXiv:1409.6887.
- ¹⁴G. Bersuker, D. C. Gilmer, D. Veksler, P. Kirsch, L. Vandelli, A. Padovani, L. Larcher, K. McKenna, A. Shluger, V. Iglesias, M. Porti, and M. Nafria, *Journal of Applied Physics* **110**, 124518 (2011).
- ¹⁵T.-H. Hou, K.-L. Lin, J. Shieh, J.-H. Lin, C.-T. Chou, and Y.-J. Lee, *Applied Physics Letters* **98**, 103511 (2011).
- ¹⁶S. Ambrogio, S. Balatti, D. C. Gilmer, and D. Ielmini, *IEEE Electron Device Lett.* **61**, 2378 (2014).
- ¹⁷C.-H. Cheng, F.-S. Yeh, and A. Chin, *Advanced Materials* **23**, 902 (2011).
- ¹⁸V. N. Kruchinin, T. V. Perevalov, V. S. Aliev, V. A. Shvets, D. R. Islamov, V. A. Gritsenko, and I. P. Prosvirin, (unpublished).
- ¹⁹K. Hübner, *Journal of Non-Crystalline Solids* **35–36, Part 2**, 1011 (1980).
- ²⁰Y. N. Novikov and V. A. Gritsenko, *Journal of Applied Physics* **110**, 014107 (2011).
- ²¹V. A. Gritsenko, R. Kwok, H. Wong, and J. B. Xu, *Journal of Non-Crystalline Solids* **297**, 96 (2002).
- ²²V. A. Gritsenko, J. B. Xu, R. W. M. Kwok, Y. H. Ng, and I. H. Wilson, *Physical Review Letters* **81**, 1054 (1998).
- ²³V. Afanas'ev, *Internal Photoemission Spectroscopy: Principles and Applications* (Elsevier Science, Amsterdam, 2008) p. 312.
- ²⁴B. I. Shklovskii, *Soviet Physics of Semiconductors* **13**, 53 (1979).
- ²⁵B. I. Shklovskii and A. L. Éfros, *Physics-Uspekhi* **18**, 845 (1975).
- ²⁶D. R. Islamov, V. A. Gritsenko, C. H. Cheng, and A. Chin, *Applied Physics Letters* **99**, 072109 (2011).
- ²⁷T. Ando, N. D. Sathaye, K. V. R. M. Murali, and E. A. Cartier, *IEEE Electron Device Lett.* **32**, 865 (2011).
- ²⁸Y. N. Novikov, *Journal of Applied Physics* **113**, 024109 (2013).
- ²⁹A. V. Shaposhnikov, T. V. Perevalov, V. A. Gritsenko, C. H. Cheng, and A. Chin, *Applied Physics Letters* **100**, 243506 (2012).
- ³⁰A. Mehonic, S. Cuff, M. Wojdak, S. Hudziak, O. Jambois, C. Labb, B. Garrido, R. Rizk, and A. J. Kenyon, *Journal of Applied Physics* **111**, 074507 (2012).